LBL-34617
UC-401
Preprint

Lawrence Berkeley Laboratory

UNIVERSITY OF CALIFORNIA

CHEMICAL SCIENCES DIVISION

Submitted to Chemical Engineering Science

Liquid-Liquid Phase Diagrams for Binary Polymer Solutions from a Perturbed Hard-Sphere-Chain Equation of State

Y. Song, S.M. Lambert, and J.M. Prausnitz

September 1993

Prepared for the U.S. Department of Energy under Contract Number DE-AC03-76SF0009

REFERENCE COPY
Does Not
Circulate
Bldg. 50 Library.
LBL-34617
Copy 1

DISCLAIMER

This document was prepared as an account of work sponsored by the United States Government. While this document is believed to contain correct information, neither the United States Government nor any agency thereof, nor the Regents of the University of California, nor any of their employees, makes any warranty, express or implied, or assumes any legal responsibility for the accuracy, completeness, or usefulness of any information, apparatus, product, or process disclosed, or represents that its use would not infringe privately owned rights. Reference herein to any specific commercial product, process, or service by its trade name, trademark, manufacturer, or otherwise, does not necessarily constitute or imply its endorsement, recommendation, or favoring by the United States Government or any agency thereof, or the Regents of the University of California. The views and opinions of authors expressed herein do not necessarily state or reflect those of the United States Government or any agency thereof or the Regents of the University of California.

LBL-34617

UC-401

Liquid-Liquid Phase Diagrams for Binary Polymer Solutions from a Perturbed Hard-Sphere-Chain Equation of State

Yuhua Song, Stephen M. Lambert and John M. Prausnitz

Department of Chemical Engineering
University of California

and

Chemical Sciences Division
Lawrence Berkeley Laboratory
University of California
Berkeley, CA 94720

September 1993

This work was supported by the Director, Office of Energy Research, Office of Basic Energy Sciences, Chemical Sciences Division of the U.S. Department of Energy under Contract Number DE-AC03-76SF00098. Additional funding was provided by E. I. du Pont de Nemours & Co. (Philadelphia, PA) and Koninklijke Shell (Amsterdam, The Netherlands).

Liquid-Liquid Phase Diagrams for Binary Polymer Solutions from a Perturbed Hard-Sphere-Chain Equation of State

Yuhua Song, Stephen M. Lambert and John M. Prausnitz*

Department of Chemical Engineering, University of California and Chemical Sciences Division, Lawrence Berkeley Laboratory, University of California, Berkeley, CA 94720

ABSTRACT

The perturbed-hard-sphere chain (PHSC) equation of state for multi-component mixtures is presented as a generalization from the equation of state for pure fluids. The reference term, based on Chiew's equation of state for hard-sphere chains, requires no mixing rules. Only the attractive perturbation requires van der Waals one-fluid mixing rules. Cross parameters needed in the perturbation are obtained using pure-fluid parameters and simple combining rules. The simplifying physical assumptions required to reduce the perturbation term to the Flory χ parameter are given. Specific interactions are included by adapting the model of ten Brinke and Karasz. Model calculations for binary mixtures demonstrate that the PHSC equation can predict lower critical solution temperatures, upper critical solution temperatures and closed partial-miscibility loops. Special attention is given to the effects of polymer molecular weight, pressure, differences in segment size and differences in segment interaction energy.

1. INTRODUCTION

Molecular-based thermodynamic models for describing liquid-liquid equilibria (LLE) in polymer mixtures can be divided into four categories, each corresponding to a particular statistical mechanical framework: incompressible-lattice models, generalized van der Waals partition-function theories, compressible-lattice models, and off-lattice (continuous-space) models of chain fluids.

* To whom correspondence should be addressed.
Submitted to *Chemical Engineering Science Symposium in Print on Molecular Modelling*, September 1993.

The most widely used and best-known of the incompressible lattice models is the Flory-Huggins theory (Flory, 1953) which illustrates in a simple way the competition between the entropy of mixing and the attractive forces that produces liquid-liquid phase separation at low temperatures with an upper critical solution temperature (UCST). Much work has been done to improve the mathematical solution of the lattice problem including chain connectivity and nonrandom mixing (Guggenheim, 1952); pursuing a formal "exact" solution to the lattice problem using advanced statistical-mechanical methods (Dudowicz and Freed, 1990; Madden, *et al.*, 1990; Pesci and Freed, 1989); or using lattice Monte-Carlo simulations (Lambert, *et al.*, 1993; Szleifer, 1990). These improvements provide better agreement with experiment by widening the liquid-liquid coexistence curve.

However, polymer mixtures display more complex behavior in the liquid phase (Rowlinson and Swinton, 1982) than can be explained by the incompressible lattice. Such behavior includes limited miscibility at high temperatures with a lower critical solution temperature (LCST). Also, specific interactions can cause a homogeneous phase to reappear at temperatures below the UCST forming closed partial-miscibility loops (Bae, *et al.*, 1991). UCSTs and LCSTs can merge to exhibit hourglass-shaped phase diagrams upon decreasing pressure (Zeman and Patterson, 1972) or increasing polymer molecular weight (Siow, *et al.*, 1972). By modifying the Flory χ parameter, it is possible to determine the mathematical conditions which give rise the these types of phase diagrams. These modifications usually require giving empirical or semi-empirical dependencies of χ on temperature (Cheluget, *et al.*, 1993), temperature and composition (Bae, *et al.*, 1993; Qian, *et al.*, 1991a; Qian, *et al.*, 1991b; Solc and Koningsveld, 1992), or temperature, composition and pressure (van Opstal and Koningsveld, 1992a; 1992b).

To understand high-temperature LCSTs properly, it was recognized that free-volume effects must be included (Patterson, 1969). This is an important recognition because incompressible lattice theories cannot represent excess volumes of mixing. Early theories which attempted to include free-volume effects were based on a generalized form of the van der Waals

partition function, which is the product of two independent partition functions: one accounts for free-volume and the other for attractive forces (Flory, 1965; Flory, *et al.*, 1964). The free-volume contribution is usually based on a "cell" model, where the polymer segment occupies a cell whose volume is always larger than the "hard-core" volume of the segment (Prigogine, *et al.*, 1957). The contribution from attractive forces is determined by counting pair interactions in a manner similar to that used for the incompressible lattice; however, the "lattice energy" is assumed to be inversely proportional to some power of the volume. Since the energy is based on lattice ideas, nonrandomness has also been incorporated (Brandani, *et al.*, 1991; McMaster, 1973; Xie, *et al.*, 1992). The Perturbed Hard-Chain Theory and related equations of state (Beret and Prausnitz, 1975; Donohue and Prausnitz, 1978; Sako, *et al.*, 1989; Vimalchand and Donohue, 1989) are based on similar ideas.

Alternatively, the free-volume concept has also been included using compressible lattice models (Sanchez and Lacombe, 1976; 1978). The assumptions are the same as those for the incompressible lattice in the Flory-Huggins approximation, but vacant sites are added as an additional component. The number of vacant sites is determined by minimization of the Gibbs energy with respect to volume yielding a "lattice-fluid" equation of state. Other variations on the lattice-fluid model utilize solutions to the lattice model in the Guggenheim approximation (Costas and Sanctuary, 1981), the quasichemical approximation (High and Danner, 1989; High and Danner, 1990; Panayioutou and Vera, 1982), and more recently the Lattice-Cluster approximation (Dudowicz and Freed, 1991a; 1991b; 1991c; 1992). By using essentially lattice-based methods for counting polymer configurations and segmental interactions, all of the above-mentioned theories ignore the continuous nature of real polymer configurations.

Recent publications indicate increased interest in developing off-lattice (continuous-space), statistical-mechanical based equations of state for polymer mixtures. A rigorous statistical-mechanical treatment for polymers is difficult due to their asymmetric structure, large number of internal degrees of freedom, and strong coupling between intra- and intermolecular interactions.

Fortunately, a number of studies have focused on a relatively simple model—athermal hard-sphere chains pictured as a series of freely-jointed tangent hard spheres (Chapman, *et al.*, 1988; Chiew, 1990; Dickman and Hall, 1986; Honnell and Hall, 1989). Despite their relative simplicity, the properties of hard-sphere chains take into account some significant features of real polymer liquids, including excluded-volume effects and segment connectivity. More important, they provide a useful reference system in statistical-mechanical perturbation theories for chain-like molecular fluids, to replace the much simpler hard-sphere reference system used in most existing perturbation theories of fluids, such as the Barker-Henderson theory (Barker and Henderson, 1967), the Weeks-Chandler-Andersen theory (Weeks, *et al.*, 1971) and their modifications.

Dickman and Hall were the first to present an equation of state for hard-sphere chains (Dickman and Hall, 1986). They obtained the pressure through the formulation of chain-segment insertion probabilities in a manner analogous to that used to derive the lattice-based Flory-Huggins theory. Later, Honnell and Hall derived a new equation of state utilizing the Carnahan-Starling equation (Carnahan and Starling, 1969) and the Tildesley-Streett (Tildesley and Streett, 1980) dimer equation (Honnell and Hall, 1989). These equations have been tested against computer-simulation results for hard-sphere chains (Dickman and Hall, 1988) and their binary mixtures (Honnell and Hall, 1991). Yethiraj and Hall also extended the above equations to include square-well chains where unbonded segments interact through a square-well intermolecular potential (Yethiraj and Hall, 1991).

Another statistical-mechanical based equation of state for hard-sphere chains and mixtures was obtained by Chapman, *et al.* (1988) from Wertheim's first-order perturbation theory for associating fluids (Wertheim, 1987). Using this equation as a basis, the Statistical Associating Fluid Theory (SAFT) was developed by adding a mean-field perturbation term to include attractive or dispersion forces (Chapman, *et al.*, 1990; Huang and Radosz, 1990). SAFT has been used to explain and correlate experimental *pVT* data as well as the phase behavior of primarily supercritical fluid mixtures containing polymers (Chen, *et al.*, 1992; Huang and Radosz, 1991).

A particularly elegant, yet simple, method has been presented by Chiew (1990) who studied hard-sphere chains and mixtures using the Percus-Yevick integral-equation theory coupled with chain connectivity. Analytical equations of state for hard-sphere chains and mixtures were obtained. The structure of Chiew's result is similar to the SAFT reference equation for non-associating chains in that the properties of hard-sphere chains and mixtures can be expressed in terms of the radial distribution functions of (unbonded) hard spheres and hard-sphere mixtures at contact. A major difference is that the SAFT bonding term is obtained through a low-order perturbation whereas Chiew's result is essentially exact within the assumptions of the Percus-Yevick theory. Moreover, since the hard spheres in a chain need not all have the same diameter, Chiew's theory can represent hard-sphere-chain copolymers and their mixtures where the spherical segments have different sizes.

Recently, a significant modification and generalization of Chiew's result has been made through use of the Carnahan-Starling radial distribution functions of hard spheres and hard-sphere mixtures at contact in both the bonding and non-bonding terms (Song, *et al.*, 1993a). When compared with computer simulations of hard-sphere-chain mixtures, the new equation of state gives better agreement than Chiew's original equation of state. In general, the new equation of state is expressed more succinctly and is more convenient for application.

A perturbed-hard-sphere-chain (PHSC) equation of state has been established using this new equation of state for hard-sphere chains as the reference system plus a van der Waals attractive term as the perturbation (Song, *et al.*, 1993b). Because the effective hard-sphere-diameter and attractive-energy parameters are theoretically-based functions of temperature (Song and Mason, 1989), this PHSC equation of state is applicable to fluids containing small or large molecules including polymers and copolymers.

The primary purpose of this paper is to extend to mixtures the PHSC equation of state for pure fluids described earlier (Song, *et al.*, 1993b). Unlike most existing mixture theories such as conformal-solution theories (*e.g.*, Lee, 1988), extension of the equation of state for mixtures

emerges clearly and rigorously from the theoretical nature of the equation of state for pure fluids, without the use of mixing rules for the reference part. Only the attractive term requires van der Waals one-fluid (vdW1) mixing rules which can also be derived from a first-order perturbation theory for mixtures (McQuarrie, 1976). By adopting vdW1 mixing rules, our results are essentially for a mean-field mixture.

An additional purpose of this paper is to use this equation of state for mixtures for a molecular study of liquid-liquid phase equilibria (LLE) of binary polymer solutions. In principle, however, the equation of state presented here is also applicable to vapor-liquid equilibria because it is applicable to fluid mixtures containing any number of components and over the entire range of fluid conditions. We are particularly concerned here with binary LLE because of the variety of observed liquid-liquid phase behavior reported in the literature.

The remainder of this paper is organized as follows: In Section 2, we give a short derivation of the equation of state for mixtures as a generalization from pure fluids, present a simple method for the inclusion of specific interactions and summarize the pertinent thermodynamic functions needed to calculate liquid-liquid equilibria in binary mixtures. In Section 3 we present calculated phase diagrams for model mixtures and investigate the effects of polymer molecular weight, pressure, segment size differences, and segment interaction energy differences. Conclusions are summarized in Section 4.

2. EQUATION OF STATE & THERMODYNAMIC FUNCTIONS

2.1. *Equation of State for Mixtures*

Derivation of the equation of state for mixtures follows a rigorous first-order statistical mechanical perturbation theory based on a mixture of hard-sphere chains as the reference system, and closely parallels that for pure fluids. Only the main steps need to be presented.

The equation of state for pure fluids is written (Song, *et al.*, 1993b)

$$\frac{p}{\rho k_B T} = 1 + r^2 b\rho g(d^+) - (r-1)\left[g(d^+)-1\right] - \frac{r^2 a\rho}{k_B T} \tag{2.1.1}$$

where p is the pressure, $\rho = N/V$ is the number density (N is the number of molecules and V the volume), k_B is the Boltzmann constant, T is the absolute temperature, $g(d^+)$ is the radial distribution function of hard spheres at contact and d is the effective hard-sphere diameter. In Eq. (2.1.1), the first three terms represent the reference equation of state for hard-sphere chains, and the last term is a van der Waals type perturbation to take into account attractive forces. The three segment-based parameters in Eq. (2.1.1), r, b, and a, all have a clear physical interpretation. The first parameter, r, represents the number of effective hard spheres per molecule. The second parameter, b, represents the second virial coefficient of hard spheres; it is an effective van der Waals covolume. The third parameter, a, reflects the strength of the attractive forces between two non-bonded segments. In the PHSC theory both b and a are temperature dependent; they are given by (Song, *et al.*, 1993b):

$$b(T) = \frac{2\pi}{3} d^3(T) = \frac{2\pi}{3}\sigma^3 \mathcal{F}_b\left(k_B T/\varepsilon s\right) \tag{2.1.2}$$

$$a(T) = \frac{2\pi}{3}\sigma^3 \varepsilon \mathcal{F}_a\left(k_B T/\varepsilon s\right) \tag{2.1.3}$$

where d is the effective hard-sphere diameter of a segment. The constants ε and σ are associated with a pair potential; ε is the depth of the minimum in the pair potential and σ is the separation distance between segment centers at this minimum. (The definition of σ used here differs from its usual definition as the separation distance between segment centers when the potential is zero.) Alternatively, σ can be considered an effective "hard-core" segment diameter at absolute zero temperature. In Eqs. (2.1.2) and (2.1.3), $\mathcal{F}_a$ and $\mathcal{F}_b$ are two universal functions in terms of a scaled temperature, $k_B T/\varepsilon s$. The factor, $s(r)$, arises from the scaling of $\mathcal{F}_a$ and $\mathcal{F}_b$ from single-sphere systems to systems containing r tangent spheres; $s(r)$ is a function of r only. Since

accurate experimental values for ε and σ exist for methane and argon, the thermodynamic properties of these two fluids are used to determine the single-sphere universal functions.

Extension of Eq. (2.1.1) to mixtures is straightforward:

$$\begin{aligned}\frac{p}{\rho kT} &= \left(\frac{p}{\rho kT}\right)_{ref} + \left(\frac{p}{\rho kT}\right)_{pert} \\ &= 1 + \rho \sum_{ij}^{m} x_i x_j r_i r_j b_{ij} g_{ij}(d_{ij}^{+}) - \sum_{i}^{m} x_i (r_i - 1)\left[g_{ij}(d_{ij}^{+}) - 1\right] - \frac{\rho}{kT} \sum_{ij}^{m} x_i x_j r_i r_j a_{ij}\end{aligned} \tag{2.1.4}$$

where $x_i = N_i/N$ is the number fraction of molecules (effective hard-sphere chains), r_i is the number of hard spheres comprising component $i = 1,2,\ldots m$ and $g_{ij}(d_{ij}^{+})$ is the ij pair radial distribution function of hard-sphere mixtures at contact. Like Eq. (2.1.1), the first three terms in Eq. (2.1.4) represent the reference equation of state for hard-sphere-chain mixtures and the last term is a van der Waals-type perturbation for attractive forces. For each unlike pair of components $(i \neq j)$, additional parameters, b_{ij} and a_{ij}, are needed for the mixture. Their physical meanings are similar to those for pure fluids; b_{ij} is the second cross virial coefficient of hard-sphere mixtures, and a_{ij} is the parameter reflecting attractive forces between two unlike segments. A combining rule is not necessary for calculating b_{ij} because hard-sphere diameters are additive

$$d_{ij}(T) = \frac{1}{2}\left[d_i(T) + d_j(T)\right] \quad . \tag{2.1.5}$$

In Eq. (2.1.5), d_i and d_j are the effective hard-sphere diameters for pure fluids i and j at temperature T, respectively, as calculated from Eq. (2.1.2). An expression for b_{ij} follows from this additivity

$$b_{ij}(T) = \frac{2\pi}{3} d_{ij}^{3}(T) = \frac{1}{8}\left(b_i^{1/3} + b_j^{1/3}\right)^3, \qquad d_i = d_{ii} \quad . \tag{2.1.6}$$

Parameter a_{ij} can be obtained by extending Eq. (2.1.3) to mixtures

$$a_{ij}(T) = \frac{2\pi}{3} \sigma_{ij}^{3} \varepsilon_{ij} \mathcal{F}_{ij}(T) \tag{2.1.7}$$

where, like in pure fluids, ε_{ij} and σ_{ij} are associated with a pair potential between unlike segments. ε_{ij} and σ_{ij} can be determined from pure-component parameters using appropriate combining rules

$$\varepsilon_{ij} = \sqrt{\varepsilon_{ii}\,\varepsilon_{jj}}\,(1-k_{ij}) \tag{2.1.8}$$

$$\sigma_{ij} = \frac{\sigma_{ii}+\sigma_{jj}}{2} \quad . \tag{2.1.9}$$

Eq. (2.1.8) introduces the binary parameter, k_{ij}. In Eq. (2.1.7), $\mathcal{F}_{ij}\,(T)$ represents a temperature dependence for a_{ij}; a simple choice for $\mathcal{F}_{ij}\,(T)$ is a geometric mean of the universal function $\mathcal{F}_a$ for pure fluids i and j

$$\mathcal{F}_{ij}\,(T) = \sqrt{\mathcal{F}_a\left(\frac{k_B T}{\varepsilon_{ii}\,s(r_i)}\right)\mathcal{F}_a\left(\frac{k_B T}{\varepsilon_{jj}\,s(r_j)}\right)} \quad . \tag{2.1.10}$$

Finally, to obtain a complete equation of state from Eq. (2.1.4), a suitable mathematical form for $g_{ij}(d_{ij}^{+})$ is needed. The best known analytical expression for $g_{ij}(d_{ij}^{+})$ is the Boublik-Mansoori-Carnahan-Starling (BMCS) equation for hard-sphere mixtures (Boublik, 1970; Mansoori, *et al.*, 1971)

$$g_{ij}(\eta,\xi_{ij}) = \frac{1}{1-\eta} + \frac{3}{2}\frac{\xi_{ij}}{(1-\eta)^2} + \frac{1}{2}\frac{\xi_{ij}^2}{(1-\eta)^3} \tag{2.1.11}$$

where η is the packing fraction

$$\eta = \frac{\rho}{4}\sum_i^m x_i\,r_i\,b_i \tag{2.1.12}$$

$$\xi_{ij} = \left(\frac{b_i\,b_j}{b_{ij}}\right)^{1/3}\frac{\rho}{4}\sum_k^m x_k\,r_k\,b_k^{2/3} \quad . \tag{2.1.13}$$

For one-component systems and equal-segment-size mixtures, $\xi_{ij}=\eta$, and Eq. (2.1.11) reduces to the Carnahan-Starling equation for hard spheres.

In summary, the most notable feature of the proposed equation of state for mixtures, Eq. (2.1.4), is that the reference equation of state for hard-sphere-chain mixtures follows a rigorous statistical-mechanical theory, without using mixing rules. Only the attractive term requires van der Waals one-fluid mixing rules.

2.2 *Thermodynamic functions*

Since the equation of state is established, other thermodynamic functions, such as the Helmholtz energy and the chemical potential, can be derived. It is useful to transform Eq. (2.1.4) from *number* basis (where the independent, intensive variables are T, ρ and x_i) to *segment* basis with more useful independent variables for polymer mixtures. The segment-basis independent variables are temperature T, segment density $\rho_r = N_r/V$, and segment fraction $\phi_i = N_i r_i / N_r$ where N_r is the total number of segments in the system

$$N_r = \sum_i^m N_i r_i \quad . \tag{2.2.1}$$

The relation between x_i and ϕ_i is

$$x_i = \frac{(\phi_i/r_i)}{\sum_j^m (\phi_j/r_j)}, \qquad \text{or} \qquad \phi_i = \frac{x_i r_i}{\sum_j^m x_j r_j} \quad . \tag{2.2.2}$$

In terms of T, ρ_r, and ϕ_i, Eq. (2.1.4) can be rewritten as

$$\frac{p}{\rho_r k_B T} = 1 + \rho_r \sum_{ij}^m \phi_i \phi_j b_{ij} g_{ij}(d_{ij}^+) - \sum_i^m \phi_i \left(1 - \frac{1}{r_i}\right) g_{ij}(d_{ij}^+) - \frac{\rho_r}{k_B T} \sum_{ij}^m \phi_i \phi_j a_{ij} \quad . \tag{2.2.3}$$

The general equation for calculating the Helmholtz energy from a pressure-explicit equation of state is (Prausnitz, *et al.*, 1986)

$$A(T,V,N_i) = \sum_i^m A_i^o(T) + \int_V^\infty \left(p - \frac{N k_B T}{V}\right) dV + k_B T \sum_i^m N_i \ln\left(\frac{N_i k_B T}{V}\right) \quad . \tag{2.2.4}$$

Eq. (2.2.4) can be written in terms of T, ρ_r, and ϕ_i:

$$\frac{A}{N_r k_B T} = \sum_i^m \frac{\phi_i}{r_i} \frac{A_i^o}{N_i k_B T} + \int_0^{\rho_r} \left(\frac{p}{\rho_r k_B T} - \frac{N}{N_r} \right) \frac{d\rho_r}{\rho_r} + \sum_i^m \frac{\phi_i}{r_i} \ln\left(\frac{\phi_i}{r_i} \rho_r k_B T \right) \quad . \tag{2.2.5}$$

The final result is

$$\begin{aligned} \frac{A}{N_r k_B T} &= \sum_{i=1}^m \frac{\phi_i}{r_i} \frac{A_i^o}{N_i k_B T} + \rho_r \sum_{i,j=1}^m \phi_i \phi_j b_{ij} W_{ij} - \sum_{i=1}^m \phi_i \left(1 - \frac{1}{r_i} \right) Q_{ii} \\ &\quad - \frac{\rho_r}{k_B T} \sum_{i,j=1}^m \phi_i \phi_j a_{ij} + \sum_{i=1}^m \frac{\phi_i}{r_i} \ln\left(\frac{\phi_i}{r_i} \rho_r k_B T \right) \end{aligned} \tag{2.2.6}$$

where

$$\begin{aligned} W_{ij} &= W_{ij}(\eta, \xi_{ij}) = \frac{1}{\rho_r} \int_0^{\rho_r} g_{ij} \, d\rho_r \\ &= \frac{I_1}{\eta} + \frac{3}{2} \frac{\xi_{ij}}{\eta^2} I_2 + \frac{1}{2} \frac{\xi_{ij}^2}{\eta^3} I_3 \end{aligned} \tag{2.2.7}$$

$$\begin{aligned} Q_{ij} &= Q_{ij}(\eta, \xi_{ij}) = \int_0^{\rho_r} (g_{ij} - 1) \frac{d\rho_r}{\rho_r} \\ &= -\ln(1-\eta) + \frac{3}{2} \frac{\xi_{ij}}{1-\eta} + \frac{1}{4} \frac{\xi_{ij}^2}{(1-\eta)^2} \end{aligned} \tag{2.2.8}$$

with

$$\eta = \frac{\rho_r}{4} \sum_i^m \phi_i b_i \tag{2.2.9}$$

$$\xi_{ij} = \left(\frac{b_i b_j}{b_{ij}} \right)^{1/3} \frac{\rho_r}{4} \sum_k^m \phi_k b_k^{2/3} \tag{2.2.10}$$

$$I_n = -I_{n-1} + \frac{1}{n-1} \frac{\eta^{n-1}}{(1-\eta)^{n-1}}, \qquad I_1 = -\ln(1-\eta) \quad . \tag{2.2.11}$$

The chemical potential can be found by differentiation of Eq. (2.2.6)

$$\mu_k = \left(\frac{\partial A}{\partial N_k} \right)_{T, \rho_r, N_{i \neq k}} \quad . \tag{2.2.12}$$

The result is

$$\frac{\mu_k}{k_B T} = \frac{\mu_k^o}{k_B T} + 2 r_k \rho_r \sum_{i=1}^{m} \phi_i b_{ik} W_{ik} + \rho_r \sum_{i,j=1}^{m} \phi_i \phi_j b_{ij} \left(N_r \frac{\partial W_{ij}}{\partial N_k} \right)$$
$$- (r_k - 1) Q_{kk} - \sum_{i=1}^{m} \phi_i \left(1 - \frac{1}{r_i} \right) \left(N_r \frac{\partial Q_{ii}}{\partial N_k} \right) \tag{2.2.13}$$
$$- \frac{2 r_k \rho_r}{k_B T} \sum_{i=1}^{m} \phi_i a_{ik} + \ln\left(\frac{\phi_k}{r_k} \rho_r k_B T \right) + 1$$

where (utilizing the chain rule of partial differentiation)

$$\left(N_r \frac{\partial W_{ij}}{\partial N_k} \right) = \left(\frac{\partial W_{ij}}{\partial \eta} \right) \left(N_r \frac{\partial \eta}{\partial N_k} \right) + \left(\frac{\partial W_{ij}}{\partial \xi_{ij}} \right) \left(N_r \frac{\partial \xi_{ij}}{\partial N_k} \right) \tag{2.2.14}$$

$$\left(N_r \frac{\partial Q_{ij}}{\partial N_k} \right) = \left(\frac{\partial Q_{ij}}{\partial \eta} \right) \left(N_r \frac{\partial \eta}{\partial N_k} \right) + \left(\frac{\partial Q_{ij}}{\partial \xi_{ij}} \right) \left(N_r \frac{\partial \xi_{ij}}{\partial N_k} \right) \tag{2.2.15}$$

and

$$\left(N_r \frac{\partial \eta}{\partial N_k} \right) = \frac{\rho_r}{4} r_k b_k \tag{2.2.16}$$

$$\left(N_r \frac{\partial \xi_{ij}}{\partial N_k} \right) = \left(\frac{b_i b_j}{b_{ij}} \right)^{1/3} \frac{\rho_r}{4} r_k b_k^{2/3} \quad . \tag{2.2.17}$$

For physical interpretation, it is useful to show the necessary conditions to reduce the perturbation to the Flory χ parameter. Towards that end, the Helmholtz energy of mixing can be divided into reference and perturbation terms

$$\frac{\Delta_{mix} A}{N_r k_B T} = \frac{\Delta_{mix} A^{ref}}{N_r k_B T} + \frac{\Delta_{mix} A^{pert}}{N_r k_B T} \quad . \tag{2.2.18}$$

In Eq. (2.2.18), the form of the reference term is identical to that based on the negative athermal entropy of mixing of hard-sphere-chain mixtures which reduces to the Flory-Huggins athermal entropy of mixing under the following conditions: 1) mixing is performed at constant temperature

and total constant volume, 2) all segment diameters must be equal and 3) the packing fractions of the pure components must be equal (Song, *et al.*, 1993a). The perturbation term is

$$\frac{\Delta_{mix}A^{pert}}{N_r k_B T} = -\frac{\rho_r}{k_B T}\sum_{ij}^{m}\phi_i \phi_j a_{ij} + \frac{1}{k_B T}\sum_{i}^{m}\phi_i a_{ii}\rho_{ri} \tag{2.2.19}$$

where $\rho_{ri} = N_i r_i / V$ is the segment density of pure component i. The above three conditions lead to the result that the segment densities of the pure components must be equal to the segment density of the mixture, *i.e.* $\rho_{ri} = \rho_r$. As a result, Eq. (2.2.19) becomes

$$\begin{aligned}\frac{\Delta_{mix}A^{pert}}{N_r k_B T} &= \frac{\rho_r}{k_B T}\left[\sum_{i}^{m}\phi_i a_{ii} - \sum_{ij}^{m}\phi_i \phi_j a_{ij}\right] \\ &= \frac{\rho_r}{k_B T}\left[\sum_{i}^{m}\phi_i (1-\phi_i) a_{ii} - \sum_{i\neq j}^{m}\phi_i \phi_j a_{ij}\right] .\end{aligned} \tag{2.2.20}$$

The first term in the brackets in Eq. (2.2.20) can be further rearranged with the result

$$\sum_{i}^{m}\phi_i (1-\phi_i) a_{ii} = \sum_{ij}^{m}\phi_i \phi_j a_{ii} - \sum_{i}^{m}\phi_i^2 a_{ii} = \frac{1}{2}\sum_{i\neq j}^{m}\phi_i \phi_j (a_{ii} + a_{jj}) . \tag{2.2.21}$$

Upon substitution into Eq. (2.2.20) yields

$$\frac{\Delta_{mix}A^{pert}}{N_r k_B T} = \frac{\rho_r}{k_B T}\sum_{i\neq j}^{m}\phi_i \phi_j \left[\frac{1}{2}(a_{ii} + a_{jj}) - a_{ij}\right] \tag{2.2.22}$$

which identifies the Flory pair-interaction parameter as

$$\chi_{ij} = \frac{\rho_r}{k_B T}\left[\frac{1}{2}(a_{ii} + a_{jj}) - a_{ij}\right] . \tag{2.2.23}$$

2.3 *Specific Interactions*

To include specific interactions such as hydrogen bonding, we use here an extension of the model by ten Brinke and Karasz (1984) which has previously been used with a lattice-fluid equation of state (Sanchez and Balazs, 1989). This model assumes that a segment of component i

interacts with a segment of component j either in a non-specific manner with an interaction energy (potential well depth) ε_{ij} or in a specific manner with interaction energy $\varepsilon_{ij} + \delta\varepsilon_{ij}$. However, the probability that the two segments are not in the proper orientation to form the specific interaction is usually much greater than the probability that two segments are in the proper orientation. Hence there is an entropic penalty for forming the specific interaction. This entropic penalty is represented by a parameter, ω_{ij}, which is the ratio of the number of orientations (degeneracy) which can form a non-specific interaction to the number of orientations which can form a specific interaction.

The total energy of interaction due only to ij pair interactions, $U_{total,ij}$, is proportional to the number of segments of type i and j in the system, N_{ri} and N_{rj}, respectively. If a fraction, f_{ij}, of the interactions are specific and the remaining interactions are non-specific,

$$\begin{aligned} U_{total,ij} &\propto -\left[(1-f_{ij})\varepsilon_{ij} N_{ri} N_{rj} \quad + \quad f_{ij}(\varepsilon_{ij}+\delta\varepsilon_{ij}) N_{ri} N_{rj}\right] \\ &\propto -N_{ri} N_{rj}(\varepsilon_{ij} + f_{ij}\delta\varepsilon_{ij}) \quad . \end{aligned} \tag{2.3.1}$$

Eq. (2.3.1) suggests that, to include specific interactions, ε_{ij} in Eqs. (2.1.2), (2.1.3) and (2.1.7) be replaced by a modified energy parameter defined as an "averaged" interaction energy

$$\bar{\varepsilon}_{ij} = \varepsilon_{ij} + f_{ij}\delta\varepsilon_{ij} \quad . \tag{2.3.2}$$

If the specific interaction occurs between the same components, Eqs. (2.1.2) and (2.1.3) become

$$b_i(T) = \frac{2\pi}{3}\sigma_{ii}^3 \mathcal{F}_b\left(\frac{k_B T}{\bar{\varepsilon}_{ii} s(r_i)}\right) \tag{2.3.3}$$

$$a_i(T) = \frac{2\pi}{3}\sigma_{ii}^3 \bar{\varepsilon}_{ii} \mathcal{F}_a\left(\frac{k_B T}{\bar{\varepsilon}_{ii} s(r_i)}\right) \quad . \tag{2.3.4}$$

For specific interactions between different components, Eqs. (2.1.7) and (2.1.10) become

$$a_{ij}(T) = \frac{2\pi}{3}\sigma_{ij}^3 \bar{\varepsilon}_{ij} \mathcal{F}_{ij}(T) \tag{2.3.5}$$

$$\mathcal{F}_{ij}(T) = \sqrt{\mathcal{F}_a\left(\frac{k_B T}{\bar{\varepsilon}_{ii}\, s(r_i)}\right)\mathcal{F}_a\left(\frac{k_B T}{\bar{\varepsilon}_{jj}\, s(r_j)}\right)} \quad . \tag{2.3.6}$$

If specific interactions occur only between different components and not between any of the pure components Eq. (2.3.6) is identical to Eq. (2.1.10), but Eq. (2.3.5) is not identical to Eq. (2.1.7).

The fraction of specific interactions is determined from a Boltzmann distribution (Hino, *et al.*, 1993; Sanchez and Balazs, 1989; ten Brinke and Karasz, 1984)

$$f_{ij} = \frac{1}{1 + \omega_{ij}\exp(-\delta\varepsilon_{ij}/kT)} \quad . \tag{2.3.7}$$

2.4 *Binary mixtures*

The phase behavior of binary polymer/solvent or polymer/polymer mixtures is distinctly different from that of simple liquid mixtures. Although the physical basis of observed experimental phenomena is well understood, it remains a challenge to demonstrate the usefulness of a molecular equation of state to reproduce observed phase diagrams. The original van der Waals equation with conventional mixing rules (Van Konyenburg and Scott, 1980) can be used to calculate, qualitatively, nearly all observed phase diagrams for binary mixtures but, because of its oversimplified basis, it cannot illustrate the effect of large volume differences between solvent and polymer on liquid-liquid equilibria of polymer solutions.

Our ultimate goal in the following paragraphs is to show that Eq. (2.2.6) can predict all types of observed liquid-liquid phase diagrams of binary polymer mixtures. Although the locus of critical lines or coexistence curves can be determined in *pressure-temperature-composition* space, the calculations shown here are in the *temperature-composition* plane at a specified pressure. Special attention is given to effects of pressure, segment-size differences, segmental interaction-energy differences, and polymer molecular weight on liquid-liquid phase diagrams.

The critical conditions for binary mixtures can be expressed as (Sadus, 1992)

$$A_{\phi\phi}p_\rho - p_\phi^2 = 0 \tag{2.4.1}$$

$$A_{\phi\phi\phi}p_\rho^3 - 3p_\phi p_{\phi\phi}p_\rho^2 + 3p_\phi^2 p_{\phi\rho}p_\rho - \left[2p_\rho + p_{\rho\rho}\right]p_\phi^3 = 0 \tag{2.4.2}$$

where

$$A_{\phi\phi} = \left(\frac{\partial^2(A/N_r kT)}{\partial\phi_1^2}\right)_{T,\rho_r} \tag{2.4.3}$$

$$A_{\phi\phi\phi} = \left(\frac{\partial^3(A/N_r kT)}{\partial\phi_1^3}\right)_{T,\rho_r} \tag{2.4.4}$$

$$p_\rho = \frac{1}{kT}\left(\frac{\partial p}{\partial\rho_r}\right)_{T,\phi_i} \tag{2.4.5}$$

$$p_{\rho\rho} = \frac{\rho_r}{kT}\left(\frac{\partial^2 p}{\partial\rho_r^2}\right)_{T,\phi_i} \tag{2.4.6}$$

$$p_\phi = \frac{1}{\rho_r kT}\left(\frac{\partial p}{\partial\phi_1}\right)_{T,\rho_r} \tag{2.4.7}$$

$$p_{\phi\phi} = \frac{1}{\rho_r kT}\left(\frac{\partial^2 p}{\partial\phi_1^2}\right)_{T,\rho_r} \tag{2.4.8}$$

$$p_{\phi\rho} = \frac{1}{kT}\left(\frac{\partial^2 p}{\partial\phi_1\,\partial\rho_r}\right)_T \quad . \tag{2.4.9}$$

The quantities on the left hand sides of Eqs. (2.4.3)-(2.4.9) are defined to be dimensionless.

To calculate coexistence curves, the necessary conditions applicable to two conjugate phases $'$ and $''$ in equilibrium are

$$T' = T'', \quad p' = p'', \quad \mu_1' = \mu_1', \quad \mu_2' = \mu_2''. \tag{2.4.10}$$

In the absence of specific interactions, reducing temperature, pressure and density by the parameters of pure-component 1 (ε_{11} and σ_{11}) isolates six quantities which must be specified to fix

completely the thermodynamic properties of the binary mixture. Two obvious parameters are the effective chain length of each component, r_1 and r_2. Four more arise from the intermolecular potential between segment pairs. Of these four, two arise from the intermolecular potential of the pure fluids. The ratio $\varepsilon_{22}/\varepsilon_{11}$ characterizes differences in intermolecular forces between segments of the same type. Similarly, the size difference between segments is characterized by the ratio σ_{22}/σ_{11}. The remaining two are binary parameters since they apply to the intermolecular potential between unlike components, $\varepsilon_{12}/\sqrt{\varepsilon_{11}\varepsilon_{22}} = 1 - k_{12}$ and σ_{12}/σ_{11}. Additivity of "hard-core" segment diameters [Eq. (2.1.9)] is used here to fix σ_{12}/σ_{11}.

Specific interactions introduce two additional parameters for each ij pair—$\delta\varepsilon_{ij}/\varepsilon_{ii}$, the increased depth in the potential well when a specific interaction is formed, and ω_{ij}, the ratio of the orientational degeneracy of the non-specific interaction to that of the specific interaction. For brevity we focus here only on specific interactions between different components in a mixture and not between non bonded segments of pure components.

In the next Section, we present calculations for model polymer mixtures and consider how these parameters influence phase behavior in mixtures at liquid-like densities. These parameters provide a molecular-level index for investigating structure-property relationships in polymer mixtures.

3. MODEL CALCULATIONS & DISCUSSION

Fig. 1(a) shows the liquid-liquid phase diagram for several polymers of varying molecular weight dissolved in their own monomers. Because the monomer and polymer segments are identical, their segment size and energetic parameters are identical and the pair interaction parameter, k_{12}, is zero. Zero pressure is chosen as a low pressure close to atmospheric pressure. The only difference is the chain length of the two components, giving LCST behavior.

Fig. 1(b) for a monomer/100-mer mixture indicates why these systems split into two liquid phases as temperature approaches the critical temperature of the solvent. In this figure, the segment densities of the coexisting phases are shown for each temperature along the binodal. In both Figs. 1(a) and 1(b), the temperature is reduced by the critical temperature of the pure solvent and in Fig. 1(b) the segment density is reduced by the critical segment density of the pure solvent. Because temperatures are below the critical temperature of the solvent and because the ratio of densities in Fig. 1(b) is always greater than unity, both phases are in the liquid state. As temperature approaches the critical temperature of the solvent, the density of the polymer-dilute phase decreases almost exponentially, whereas the density of the polymer-rich phase stays essentially constant (even though its composition changes dramatically). The preference for the solvent to form its own expanded phase is the driving force for LCST behavior.

As soon as a significantly large asymmetry in the pair interactions is introduced, both UCST and LCST behavior appear in solvent/polymer mixtures. This asymmetry can be introduced in three ways: 1) the energy-parameter ratio differs from unity, 2) the segment-size ratio differs from unity, and 3) a non-zero value for the binary interaction parameter, k_{12}. Since the a_{ij}, which depend explicitly on ε_{ij} and σ_{ij}, is related to the Flory χ parameter through Eq. (2.2.23) (albeit under a restrictive set of conditions), the above methods for introduction of asymmetry in the pair interactions is easily confirmed. Small differences in segment diameters can have a significant effect since σ_{ij} always appears to the third power.

Fig. 2(a) shows phase diagrams with both an UCST and a LCST. A non-zero value of k_{12} introduces asymmetry in the pair interactions. In addition, Fig. 2(a) shows that increasing polymer molecular weight decreases the LCST and increases the UCST. Fig. 2(b) is similar to Fig. 1(b), but the former includes densities of the coexisting phases below the UCST. Density differences play a secondary role for the UCST since the differences in density between phases are small as compared to those at temperatures above the LCST.

If the asymmetry in segment-pair interactions is sufficiently large, increasing the molecular weight can cause the UCST and LCST to overlap, producing an hourglass-type phase diagram, shown in Fig. 3.

When the asymmetry in the pair interactions is due to differences between pure-component energy parameters, pressure can have a large effect upon the type of phase diagram as illustrated in Fig. 4 for a monomer/100-mer mixtures and in Fig. 5 for a 3-mer/300-mer mixture. In Fig. 4, at pressures well above the critical pressure of the solvent, LCSTs no longer are present below the critical temperature of the solvent but UCSTs remain. As pressure falls, LCSTs decrease significantly and UCSTs increase slightly and eventually merge to form hourglass-shaped phase diagrams. Since real solvents can rarely be represented by a single sphere, Fig. 5 is included to illustrate that the same type of behavior occurs in more realistic systems at typical experimentally-accessible pressures.

In polymer blends, the entropy of mixing is very small. Therefore, small asymmetries in pair interactions can cause UCST-type partial immiscibilities as illustrated in Fig. 6 for a 1000-mer blend for three different ratios of the pure-component interaction energies close to unity. Small increases in the ratio of pure interaction energies can lead to dramatic increases in the UCST. For polymer blends, the range of the scaled temperature, $k_B T/\varepsilon_{11}$, investigated here is restricted to values less than 2.0-3.0 because typical values for the energy parameter of a pure polymer liquid are in the range of 200-700 K (Song, *et al.*, 1993b). Hence, the temperature ranges presented here are realistic. The lowest UCST in Fig. 6 is at a very low temperature, possibly below the blend's glass-transition temperature; as a result, the lowest UCST may be difficult to observe experimentally. Conversely, if asymmetries in pair interactions are large, the UCST may increase above experimentally-accessible temperatures causing incompatibility.

The usual explanation for LCST behavior in polymer blends is that the small entropy of mixing enhances the effects of small disparities in compressibilities of the two polymers (McMaster, 1973). Compressibility differences are typically related to differences in molecular

size of the polymers. In most models (particularly lattice-based models), differences in molecular size can only be reflected by differences in chain length, r. Few studies exist which also consider the effect of segment size (Kammer, 1989). In the PHSC equation of state, differences in segment size arise through the ratio of pure-component segment diameters. As illustrated in Fig. 7, differences in segment diameter (coupled with asymmetries in interaction energies) can lead to LCST-type behavior, even in mixtures where both polymers have an equal number of segments. This system also exhibits an UCST, but at a very low temperature which may be below the glass-transition temperature. Like solvent/polymer systems, LCSTs due exclusively to chain length differences were found to occur only near the critical temperature of the smaller chain-length component, which is an unmeasurably high temperature for polymers of significant molecular weight.

Closed partial-miscibility loops can be produced by inclusion of specific interactions as illustrated in Fig. 8. For illustration, this figure shows only the effects of specific interactions for a monomer mixture where the only difference between components is the 1-2 pair interaction. These types of phase diagrams occur in mixtures of highly polar fluids; to produce an UCST at a reasonable temperature, a relatively large value of k_{12} is required. The large values for $\delta\varepsilon_{12}$ (as compared to ε_{11}) and ω_{12} indicate a highly specific, energetically favorable interaction which causes a single homogeneous phase to reappear at a temperature below the UCST.

Fig. 9 illustrates the effect of polymer molecular weight on the size of the partial-miscibility loop for a solvent/polymer mixture. As the molecular weight of the polymer increases, the UCST begins to approach the critical temperature of the pure solvent whereas the LCST decreases only slightly. The critical compositions are shifted towards the pure solvent as molecular weight increases; for each molecular weight the critical composition at the UCST is slightly different from that at the LCST.

4. CONCLUSIONS

The continuous-space theory of polymer mixtures discussed here is based on a perturbation of a modified Chiew equation of state for athermal hard-sphere chains; that equation is obtained from the integral theory of fluids using the Percus-Yevick closure with a hard-sphere connectivity constraint. The perturbation is of the simple van der Waals form.

For the theory presented here, no mixing rules are required for the hard-sphere reference term. Van der Waals one-fluid theory is used for extending the perturbation to mixtures. Specific interactions, such as hydrogen bonding, are introduced through the method of ten Brinke and Karasz.

Relative to other theories, the PHSC theory has a significant advantage: the spherical segment diameter of one component need not be the same as that of another component. Further, within a given component, the segment diameters need not all be the same. It is this feature which makes the theory attractive for mixtures containing copolymers, to be discussed in a separate publication.

Phase diagrams are presented for a variety of binary polymer-solvent and polymer-polymer mixtures. Although this theory is applicable to vapor-liquid equilibria, examples illustrating liquid-liquid equilibria are presented here because liquid-liquid equilibria provide a much more critical test of the theory. Using physically reasonable parameters, the theory successfully reproduces phase diagrams with upper or lower critical solution temperatures, or both, including closed partial-miscibility loops. Attention is given to the effect of molecular weight, pressure and various molecular parameters on phase behavior.

ACKNOWLEDGMENTS

This work was supported by the Director, Office of Energy Research, Office of Basic Energy Sciences, Chemical Sciences Division of the U.S. Department of Energy under Contract No. DE-AC03-76SF00098. Additional funding was provided by E.I. duPont Nemours & Co. (Philadelphia, PA) and Koninklijke Shell (Amsterdam, The Netherlands). The authors thank Toshiaki Hino for useful discussions concerning polymer blends.

REFERENCES

Bae, Y. C., Lambert, S. M., Soane, D. S. and Prausnitz, J. M., 1991, Cloud-Point Curves of Polymer Solutions from Thermooptical Measurements. *Macromolecules* **24**, 4403-4407.

Bae, Y. C., Shim, J. J., Soane, D. S. and Prausnitz, J. M., 1993, Representation of Vapor-Liquid and Liquid-Liquid Equilibria for Binary Systems Containing Polymers: Applicability of an Extended Flory-Huggins Equation. *J. Appl. Polym. Sci.* **47**, 1193-1206.

Barker, J. A. and Henderson, D., 1967, Perturbation theory and equation of state for fluids. II. A successful theory of liquids. *J. Chem. Phys.* 4714-4721.

Beret, S. and Prausnitz, J. M., 1975, Perturbed Hard-Chain Theory: An Equation of State for Fluids Containing Small or Large Molecules. *AIChE J.* **21**, 1123-1132.

Boublik, T., 1970, Hard-sphere equation of state. *J. Chem. Phys.* **53**, 471-472.

Brandani, V., Del Re, G. and Di Giacomo, G., 1991, Flory's Equation of State for Nonrandom Polymer-Solvent Solutions. Application of Local Composition and the Two-Fluid Theory of Mixtures. *Macromolecules* **24**, 2391-2396.

Carnahan, N. F. and Starling, K. E., 1969, Equation of State for Nonattracting Rigid Spheres. *J. Chem. Phys.* **51**, 635-636.

Chapman, W. G., Gubbins, K. E., Jackson, G. and Radosz, M., 1990, New reference equation of state for associating liquids. *I & EC Res.* **29**, 1709-1721.

Chapman, W. G., Jackson, G. and Gubbins, K. E., 1988, Phase equilibria of associating fluids: Chain molecules with multiple bonding sites. *Molec. Phys.* **65**, 1057-1079.

Cheluget, E. L., Weber, M. E. and Vera, J. H., 1993, Modifications of the Flory-Huggins-Goldstein Model for Accurate Description of Closed-Loop Phase Diagrams. *Chem. Eng. Sci.* **48**, 1415-1426.

Chen, S.-J., Economou, I. G. and Radosz, M., 1992, Density-tuned polyolefin phase equilibria. 2. Multicomponent solutions of alternating poly(ethylene-propylene) in subcritical and supercritical olefins. Experiment and SAFT model. *Macromolecules* **25**, 4987-4995.

Chiew, Y. C., 1990, Percus-Yevick Integral Equation Theory for Athermal Hard-Sphere Chains. Part I: Equations of State. *Molec. Phys.* **70**, 129-143.

Costas, M. and Sanctuary, B. C., 1981, Theory of Pure *r*-mers In the Guggenheim Approximation. *J. Phys. Chem.* **58**, 3153-3160.

Dickman, R. and Hall, C. K., 1986, Equation of State for Chain Molecules: Continuous-Space Analog of Flory Theory. *J. Chem. Phys.* **85**, 4108-4115.

Dickman, R. and Hall, C. K., 1988, High density Monte Carlo simulations of chain molecules: Bulk equation of state and density profile near walls. *J. Chem. Phys.* **89**, 3168-3174.

Donohue, M. D. and Prausnitz, J. M., 1978, Perturbed Hard Chain Theory for Fluid Mixtures: Thermodynamic Properties for Mixtures in Natural Gas and Petroleum Technology. *AIChE J.* **24**, 849-860.

Dudowicz, J. and Freed, K. F., 1990, Influence of Blend Compressibility on Extapolated Zero-Angle Coherent Scattering and Spinodal: Limitations of RPA Analysis. *Macromolecules* **23**, 1519-1526.

Dudowicz, J. and Freed, K. F., 1991a, Effect of Monomer Structure and Compressibility on the Properties of Multicomponent Polymer Blends and Solutions: 1. Lattice Cluster Theory of Compressible Systems. *Macromolecules* **24**, 5076-5095.

Dudowicz, J. and Freed, K. F., 1991b, Effect of Monomer Structure and Compressibility on the Properties of Multicomponent Polymer Blends and Solutions: 2. Application to Binary Blends. *Macromolecules* **24**, 5096-5111.

Dudowicz, J. and Freed, K. F., 1991c, Effect of Monomer Structure and Compressibility on the Properties of Multicomponent Polymer Blends and Solutions: 3. Application to PS(D)/PVME Blends. *Macromolecules* **24**, 5112-5123.

Dudowicz, J. and Freed, K. F., 1992, Role of Monomer Structure and Compressibility on the Properties of Multicomponent Polymer Blends and Solutions: IV. High Molecular Weights, Temperature Dependencies, and Phase Diagrams of Binary Polymer Blends. *Theor. Chim. Acta.* **82**, 357-382.

Flory, P. J., 1953, *Principles of Polymer Chemistry*. Cornell University Press, Ithaca, N.Y.

Flory, P. J., 1965, Statisical Thermodynamics of Liquid Mixtures. *J. Phys. Chem.* **87**, 1833-1838.

Flory, P. J., Orwoll, R. A. and Vrij, A., 1964, Statistical Thermodynamics of Chain Molecule Liquids. I. An Equation of State for Normal Parrafin Hydrocarbons. *JACS* **86**, 3507-3514.

Guggenheim, E. A., 1952, *Mixtures*. Clarendon Press, Oxford.

High, M. S. and Danner, R. P., 1989, A Group Contribution Equation of State for Polymer Solutions. *Fluid Phase Eq.* **53**, 323-330.

High, M. S. and Danner, R. P., 1990, Application of the Group Contribution Lattice-Fluid EOS to Polymer Solutions. *AIChE J.* **36**, 1625-1632.

Hino, T., Lambert, S. M., Soane, D. S. and Prausnitz, J. M., 1993, Lattice Thermodynamics for Binary Closed-Loop Equilibria: Ordinary and Polymer Systems. *AIChE J.* **39**, 837-845.

Honnell, K. G. and Hall, C. K., 1989, A New Equation of State for Athermal Chains. *J. Chem. Phys.* **90**, 1841-1855.

Honnell, K. G. and Hall, C. K., 1991, Theory and simulation of hard-chain mixtures: Equations of state, mixing properties, and density profiles near hard walls. *J. Chem. Phys.* **95**, 4481-4501.

Huang, S. H. and Radosz, M., 1990, Equation of State for Small, Large, Polydisperse, and Associating Molecules. *I & EC Res.* **29**, 2284-2294.

Huang, S. H. and Radosz, M., 1991, Equation of State for Small, Large, Polydisperse, and Associating Molecules: Extension to Fluid Mixtures. *I & EC Res.* **30**, 1994-2005.

Kammer, H.-W., 1989, Upper and Lower Critical Solution Temperature Behavior in Polymer Blends and its Thermodynamic Interpretation. *Polymer* **30**, 888-892.

Lambert, S. M., Soane, D. S. and Prausnitz, J. M., 1993, Liquid-Liquid in Binary Systems: Monte-Carlo Simulations for Calculating the Effect of Nonrandom Mixing. *Fluid Phase Eq.* **83**, 59-68.

Lee, L. L., 1988, *Molecular Thermodynamics of Nonideal Fluids.* Butterworths, Boston.

Madden, W. G., Pesci, A. I. and Freed, K. F., 1990, Phase Equilibria of Lattice Polymer and Solvent: Tests of Theories Against Simulation. *Macromolecules* **23**, 1181-1191.

Mansoori, G. A., Carnahan, N. F., Starling, K. E. and Leland, T. W., 1971, Equilibrium thermodynamic properties of the mixture of hard spheres. *J. Chem. Phys.* **54**, 1523-1525.

McMaster, L. P., 1973, Aspects of Polymer-Polymer Thermodynamics. *Macromolecules* **6**, 760-773.

McQuarrie, D. A., 1976, *Statistical Mechanics.* Harper Collins Publishers, Inc., New York.

Panayioutou, C. and Vera, J. H., 1982, Statistical Thermodynamics of *r*-Mer Fluids and Their Mixtures. *Polym. J.* **14**, 681-694.

Patterson, D., 1969, Free Volume and Polymer Solubility. A Qualitative View. *Macromolecules* **2**, 672-677.

Pesci, A. I. and Freed, K. F., 1989, Lattice Theory of Polymer Blends and Liquid Mixtures: Beyond the Flory-Huggins Approximation. *J. Chem. Phys.* **90**, 2017-2026.

Prausnitz, J. M., Lichtenthaler, R. N. and Azevedo, E. G. d., 1986, *Molecular Thermodynamics of Fluid Phase Equilibria.* Prentice-Hall Inc., Englewood Cliffs, N.J.

Prigogine, I., Bellemans, A. and Mathot, V., 1957, *The Molecular Theory of Solutions.* North-Holland Publishing Company, Amsterdam.

Qian, C., Mumby, S. J. and Eichinger, B. E., 1991a, Existence of Two Critical Concentrations in Binary Phase Diagrams. *J. Polym. Sci.: Pt. B: Polym. Phys.* **29**, 635-637.

Qian, C., Mumby, S. J. and Eichinger, B. E., 1991b, Phase Diagrams of Polymer Solutions and Blends. *Macromolecules* **24**, 1655-1661.

Rowlinson, J. S. and Swinton, F. L., 1982, *Liquids and Liquid Mixtures.* Butterworths, Boston.

Sadus, R. J., 1992, *High Pressure Phase Behavior of Multicomponent Fluid Mixtures.* Elsevier Science Publishers B.V., Amsterdam.

Sako, T., Wu, A. H. and Prausnitz, J. M., 1989, A Cubic Equation of State for High-Pressure Phase Equilibria of Mixtures Containing Polymers and Volatile Fluids. *J. Appl. Polym. Sci.* **38**, 1839-1858.

Sanchez, I. C. and Balazs, A. C., 1989, Generalization of the Lattice-Fluid Model for Specific Interactions. *Macromolecules* **22**, 2325-2331.

Sanchez, I. C. and Lacombe, R. H., 1976, Statistical Thermodynamics of Fluid Mixtures. *J. Phys. Chem.* **80**, 2568-2580.

Sanchez, I. C. and Lacombe, R. H., 1978, Statistical Thermodynamics of Polymer Solutions. *Macromolecules* **11**, 1145-1156.

Siow, K. S., Delmas, G. and Patterson, D., 1972, Cloud-Point Curves in Polymer Solutions with Adjacent Upper and Lower Critical Solution Temperatures. *Macromolecules* **5**, 29-34.

Solc, K. and Koningsveld, R., 1992, Coalescence of Upper and Lower Miscibility Gaps in Systems with Concentration-Dependent Interactions. *J. Phys. Chem.* **96**, 4056-4068.

Song, Y., Lambert, S. M. and Prausnitz, J. M., 1993a, Equations of State for Hard-Sphere Chain Mixtures. Submitted to *Macromolecules.*

Song, Y., Lambert, S. M. and Prausnitz, J. M., 1993b, A Perturbed-Hard-Sphere-Chain Equation of State for Normal Liquids or Polymers. Submitted to *AIChE Journal.*

Song, Y. and Mason, E. A., 1989, Statistical-mechanical theory of a new analytical equation of state. *J. Chem. Phys.* **91**, 7840-7853.

Szleifer, I., 1990, A New Mean-Field Theory for Dilute Polymer Solutions: Phase Diagram, Conformational Behavior and Interfacial Properties. *J. Chem. Phys.* **92**, 6940-6952.

ten Brinke, G. and Karasz, F. E., 1984, Lower Critical Solution Temperature Behavior in Polymer Blends: Compressibility and Directional-Specific Interactions. *Macromolecules* **17**, 815-820.

Tildesley, D. J. and Streett, W. B., 1980, An Equation of State for Hard Dumbell Fluids. *Molec. Phys.* **41**, 85-94.

Van Konyenburg, P. H. and Scott, R. L., 1980, Critical Lines and Phase Equilibria in Binary van der Waals Mixtures. *Phil. Trans. R. Soc. London A* **298**, 495-540.

van Opstal, L. and Koningsveld, R., 1992a, Mean-field Lattice Equations of State: 4. Influence of Pressure on Liquid-Liquid Phase Behavior of Polymer Blends. *Polymer* **33**, 3445-3452.

van Opstal, L. and Koningsveld, R., 1992b, Mean-field Lattice Equations of State: 4. Influence of Pressure on the Phase Behavior of the System Polystyrene/Cyclohexane. *Polymer* **33**, 3433-3444.

Vimalchand, P. and Donohue, M. D., 1989, Comparison of Equations of State for Chain Molecules. *J. Phys. Chem.* **93**, 4355-4360.

Weeks, J. D., Chandler, D. and Andersen, J., 1971, Role of repulsive forces in determining the equilibrium structure of simple liquids. *J. Chem. Phys.* **54**, 5237-5247.

Wertheim, M. S., 1987, Thermodynamic perturbation theory of polymerlization. *J. Chem. Phys.* **87**, 7323-7331.

Xie, H., Nies, E., Stroeks, A. and Simha, R., 1992, Some Considerations on Equation of State and Phase Relations: Polymer Solutions and Blends. *Polymer Engineering and Science* **32**, 1654-1664.

Yethiraj, A. and Hall, C. K., 1991, Generalized Flory equations of state for square-well chains. *J. Chem. Phys.* **95**, 8494-8506.

Zeman, L. and Patterson, D., 1972, Pressure Effects in Polymer Solutions Phase Equilibria. II. Systems Showing Upper and Lower Solution Temperatures. *J. Phys. Chem.* **76**, 1214-1219.

FIGURE CAPTIONS

Figure 1. (a) Liquid-Liquid phase diagram for several different-chain length polymers mixed with their monomers. Since the polymer segments are identical to the monomer only LCST behavior is observed at high temperatures approaching the critical temperature of the pure monomer. (b) Segment densities of coexisting phases along the binodal for a monomer/100-mer mixture.

Figure 2. (a) Monomer/polymer mixtures exhibiting both UCST and LCST behavior. As the molecular weight of the polymer rises the LCST decreases and the UCST increases. (b) The segment densities of coexisting phases along both binodals for a monomer/100-mer mixture. The difference in segment densities for the LCST curve is large opposed to that for the UCST curve.

Figure 3. Phase diagram for monomer/polymer mixtures where the UCST and LCST merge to form an hourglass-type phase diagram upon increasing the polymer molecular weight.

Figure 4. The effect of pressure on the phase diagram for a monomer/100-mer mixture. As pressure falls towards "atmospheric" pressure, the UCST and LCST can merge to form hourglass type phase diagrams. At high pressures (well above the critical pressure of the monomer), the LCST increases above the critical temperature of the pure monomer, but the UCST changes only slightly.

Figure 5. The effect of pressure on the phase diagram for a 3-mer/300-mer mixture. This figure represents a more realistic solvent at pressures that are accessible experimentally.

Figure 6. Phase diagram for a 1000-mer blend exhibiting only an UCST. With small increases in the ratio of the interaction energies between segments of the same type, there is a large increase in the UCST.

Figure 7. Phase diagram for a 1000-mer blend exhibiting both an UCST and a LCST. The LCST arises from differences in segment size coupled with asymmetries in pair interactions.

Figure 8. Phase diagram for a monomer/monomer mixture exhibiting a closed partial-miscibility loop. Both monomers are identical except for the 1-2 pair interaction (which includes a specific interaction) and as a result, produces a phase diagram which is symmetric about $x_1 = x_2 = 1/2$.

Figure 9. Effect of polymer molecular weight on the phase diagrams of solvent/polymer mixtures exhibiting closed partial-miscibility loops. Specific interactions only occur between different components. For each molecular weight, the composition at the UCST is slightly different from that at the LCST.

Figure 1

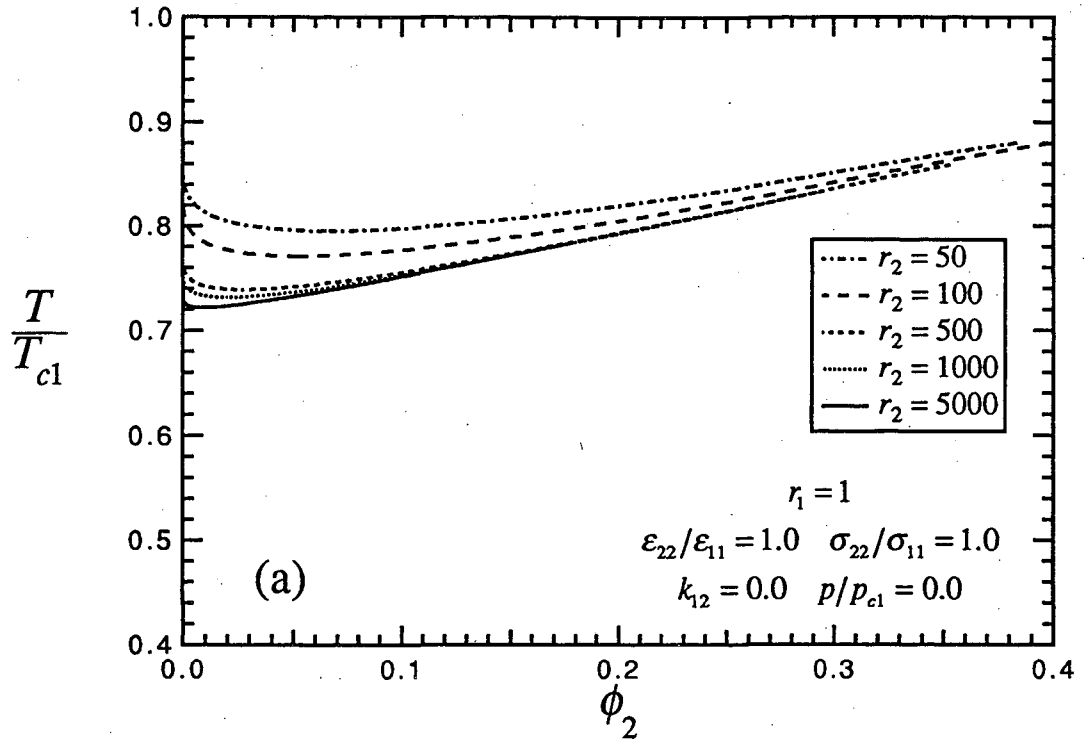
1.0
0.9
0.8
0.7
0.6
0.5
0.4
0.0
0.1
0.2
0.3
0.4
$\frac{T}{T_{c1}}$
ϕ_2
$r_2 = 50$
$r_2 = 100$
$r_2 = 500$
$r_2 = 1000$
$r_2 = 5000$
$r_1 = 1$
$\varepsilon_{22}/\varepsilon_{11} = 1.0 \quad \sigma_{22}/\sigma_{11} = 1.0$
$k_{12} = 0.0 \quad p/p_{c1} = 0.0$
(a)

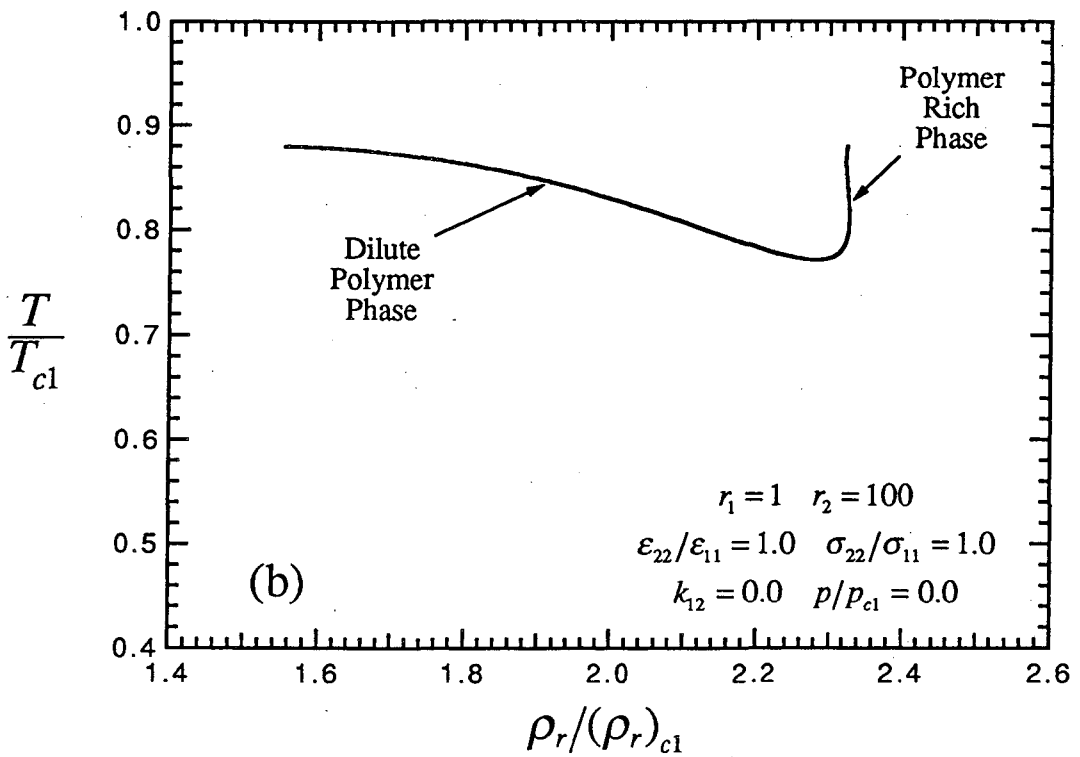
1.0
0.9
0.8
0.7
0.6
0.5
0.4
1.4
1.6
1.8
2.0
2.2
2.4
2.6
$\frac{T}{T_{c1}}$
$\rho_r/(\rho_r)_{c1}$
Polymer Rich Phase
Dilute Polymer Phase
$r_1 = 1 \quad r_2 = 100$
$\varepsilon_{22}/\varepsilon_{11} = 1.0 \quad \sigma_{22}/\sigma_{11} = 1.0$
$k_{12} = 0.0 \quad p/p_{c1} = 0.0$
(b)

Figure 2

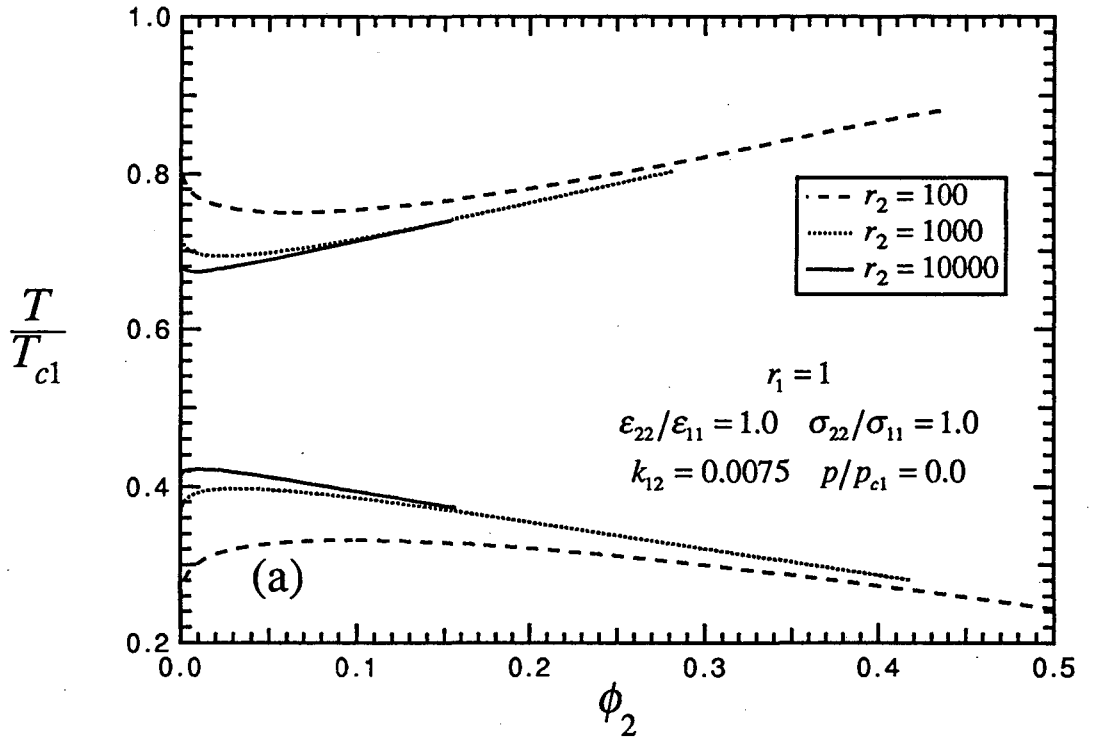
1.0
0.8
0.6
0.4
0.2
0.0
0.1
0.2
0.3
0.4
0.5
$\frac{T}{T_{c1}}$
ϕ_2
$r_2 = 100$
$r_2 = 1000$
$r_2 = 10000$
$r_1 = 1$
$\varepsilon_{22}/\varepsilon_{11} = 1.0 \quad \sigma_{22}/\sigma_{11} = 1.0$
$k_{12} = 0.0075 \quad p/p_{c1} = 0.0$
(a)

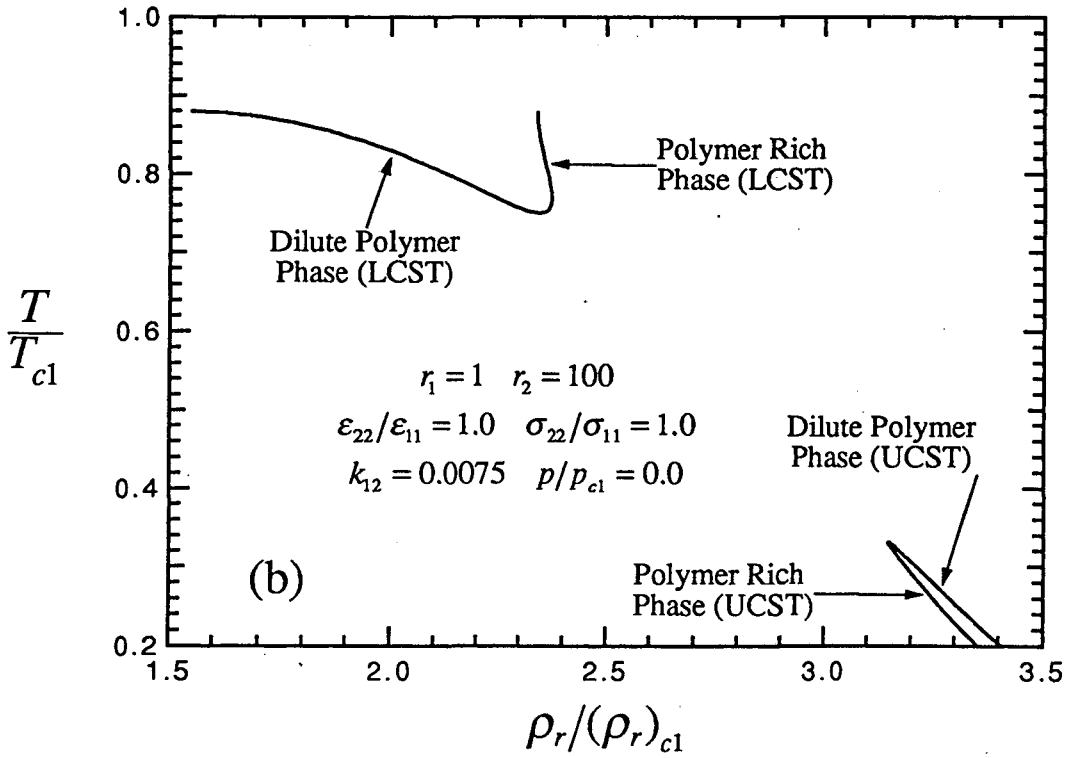
1.0
0.8
0.6
0.4
0.2
1.5
2.0
2.5
3.0
3.5
$\frac{T}{T_{c1}}$
$\rho_r/(\rho_r)_{c1}$
Polymer Rich Phase (LCST)
Dilute Polymer Phase (LCST)
$r_1 = 1 \quad r_2 = 100$
$\varepsilon_{22}/\varepsilon_{11} = 1.0 \quad \sigma_{22}/\sigma_{11} = 1.0$
$k_{12} = 0.0075 \quad p/p_{c1} = 0.0$
Dilute Polymer Phase (UCST)
Polymer Rich Phase (UCST)
(b)

Figure 3

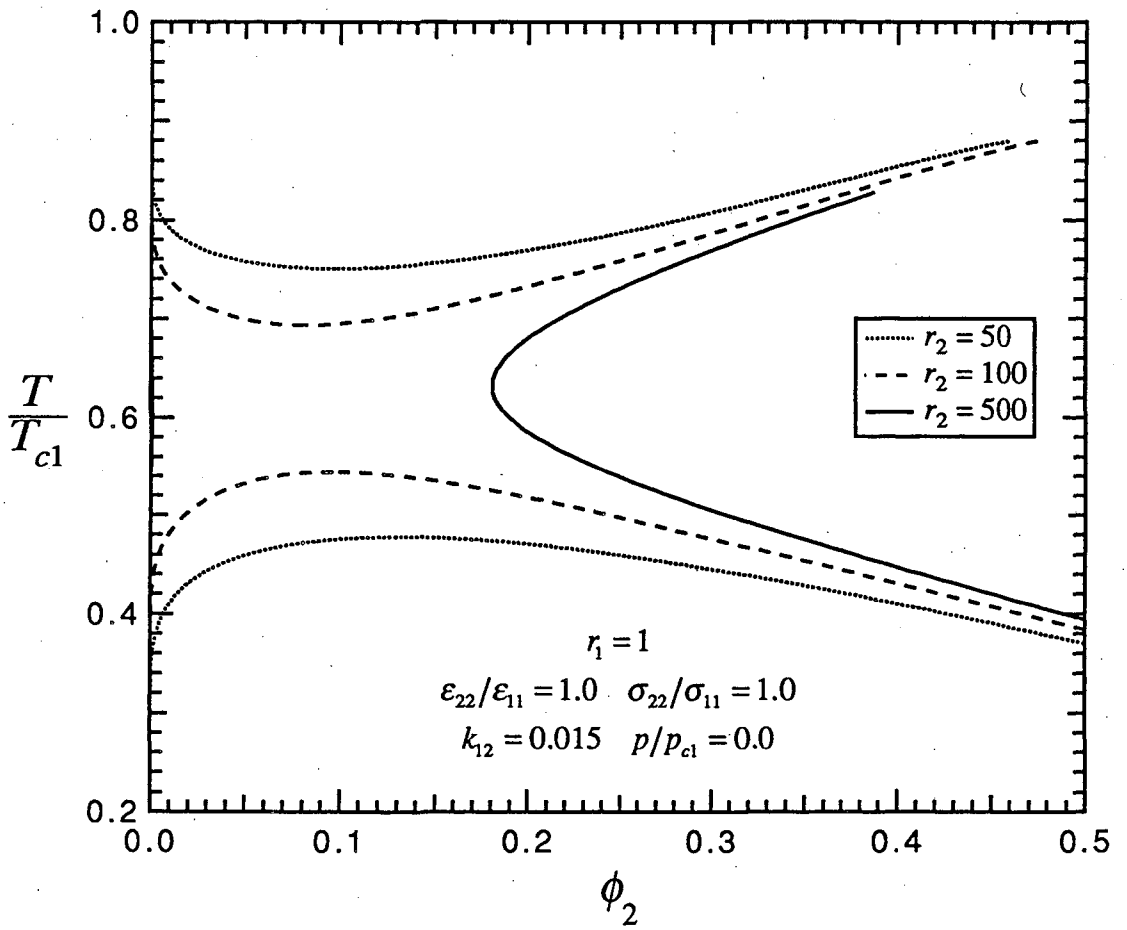
1.0
0.8
0.6
0.4
0.2
$\frac{T}{T_{c1}}$
0.0
0.1
0.2
0.3
0.4
0.5
ϕ_2
$r_2 = 50$
$r_2 = 100$
$r_2 = 500$
$r_1 = 1$
$\varepsilon_{22}/\varepsilon_{11} = 1.0 \quad \sigma_{22}/\sigma_{11} = 1.0$
$k_{12} = 0.015 \quad p/p_{c1} = 0.0$

Figure 4

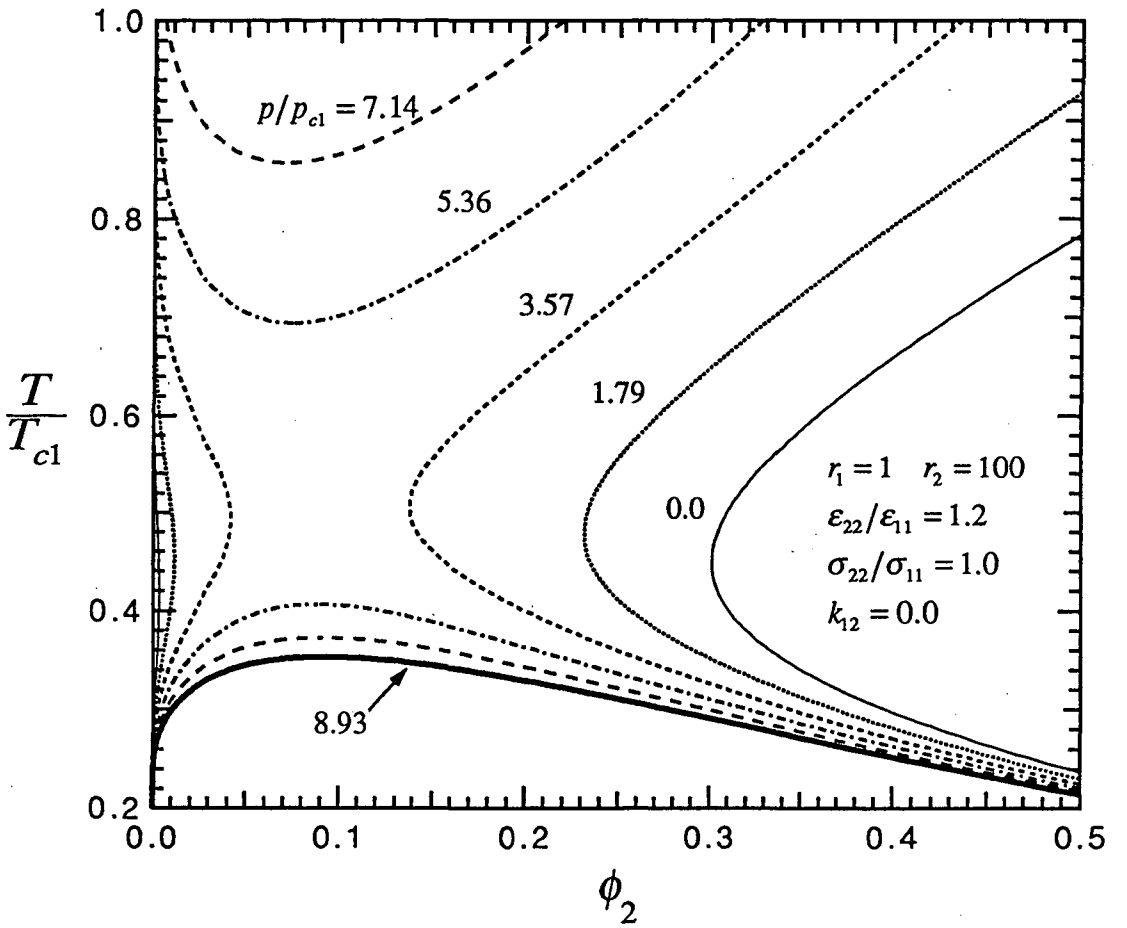
1.0
0.8
0.6
0.4
0.2
0.0
0.1
0.2
0.3
0.4
0.5
$\frac{T}{T_{c1}}$
ϕ_2
$p/p_{c1} = 7.14$
5.36
3.57
1.79
0.0
8.93
$r_1 = 1 \quad r_2 = 100$
$\varepsilon_{22}/\varepsilon_{11} = 1.2$
$\sigma_{22}/\sigma_{11} = 1.0$
$k_{12} = 0.0$

Figure 5

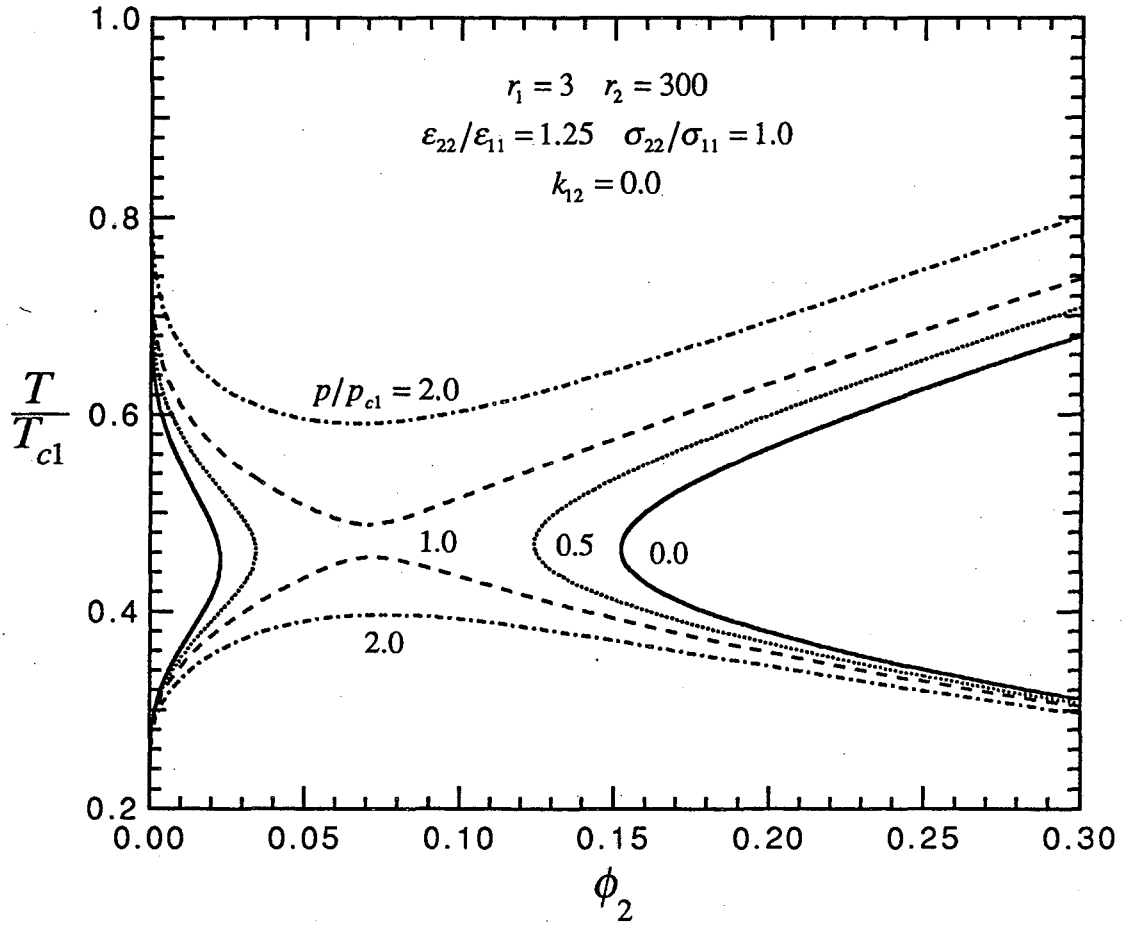
$r_1 = 3 \quad r_2 = 300$
$\varepsilon_{22}/\varepsilon_{11} = 1.25 \quad \sigma_{22}/\sigma_{11} = 1.0$
$k_{12} = 0.0$
$p/p_{c1} = 2.0$
1.0
0.5
0.0
2.0
$\frac{T}{T_{c1}}$
ϕ_2
1.0
0.8
0.6
0.4
0.2
0.00
0.05
0.10
0.15
0.20
0.25
0.30

Figure 6

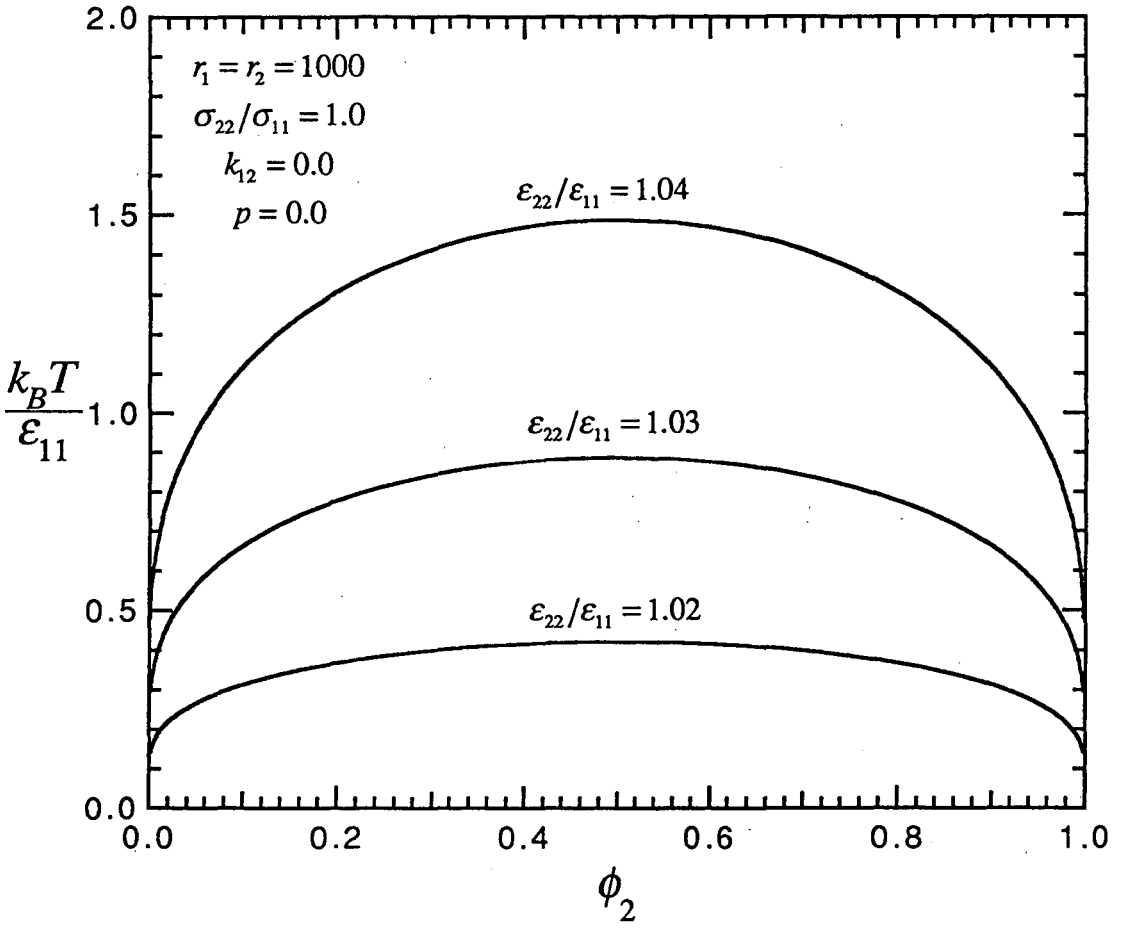
$r_1 = r_2 = 1000$
$\sigma_{22}/\sigma_{11} = 1.0$
$k_{12} = 0.0$
$p = 0.0$
$\varepsilon_{22}/\varepsilon_{11} = 1.04$
$\varepsilon_{22}/\varepsilon_{11} = 1.03$
$\varepsilon_{22}/\varepsilon_{11} = 1.02$
$\frac{k_B T}{\varepsilon_{11}}$
ϕ_2
0.0
0.5
1.0
1.5
2.0
0.0
0.2
0.4
0.6
0.8
1.0

Figure 7

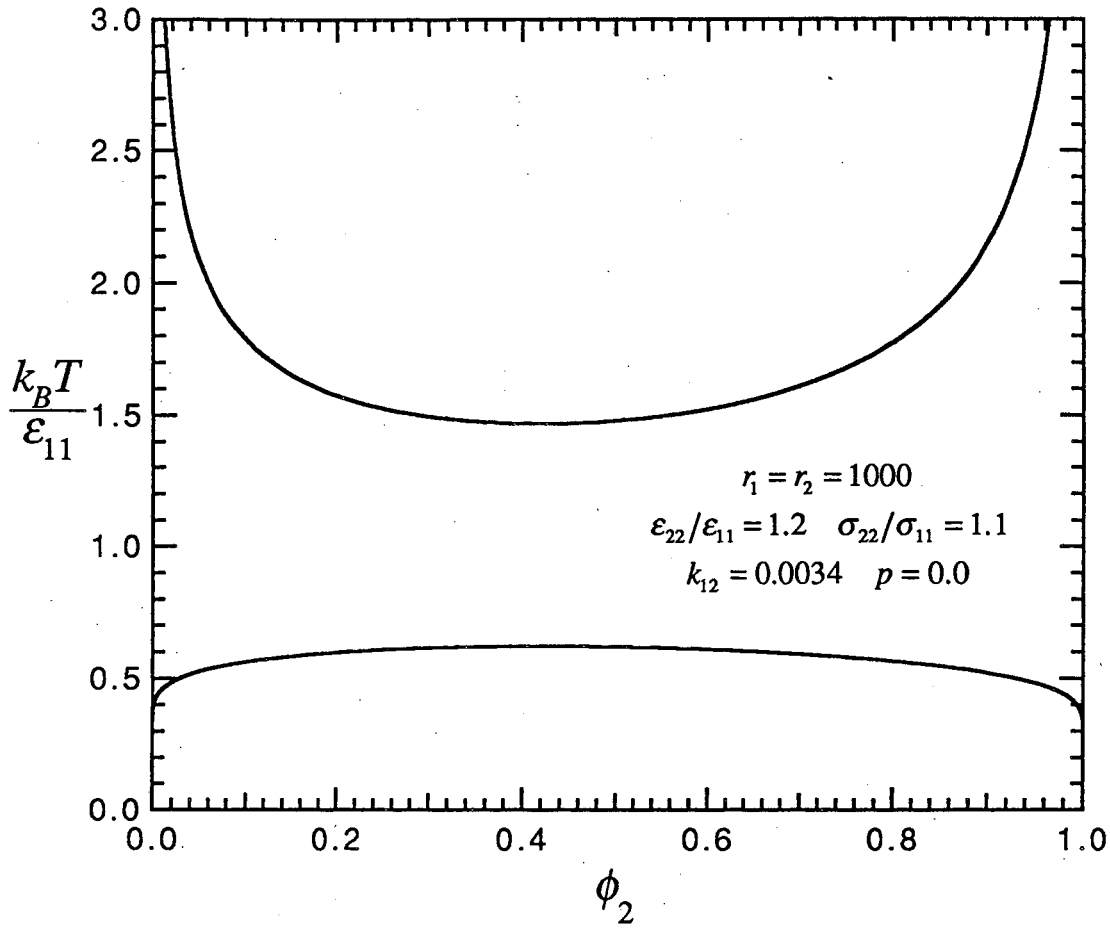
3.0
2.5
2.0
1.5
1.0
0.5
0.0
$\frac{k_B T}{\varepsilon_{11}}$
$r_1 = r_2 = 1000$
$\varepsilon_{22}/\varepsilon_{11} = 1.2 \quad \sigma_{22}/\sigma_{11} = 1.1$
$k_{12} = 0.0034 \quad p = 0.0$
0.0
0.2
0.4
0.6
0.8
1.0
ϕ_2

Figure 8

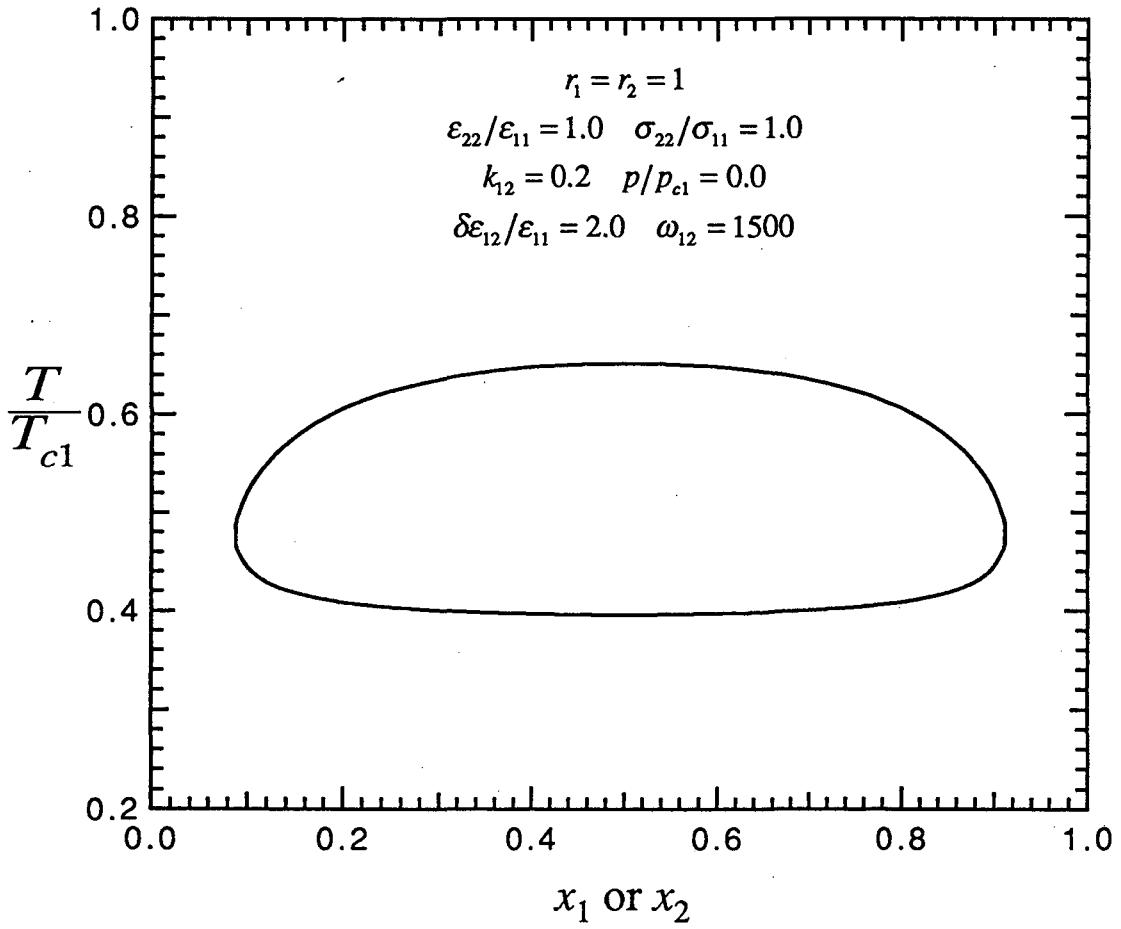
$r_1 = r_2 = 1$
$\varepsilon_{22}/\varepsilon_{11} = 1.0 \quad \sigma_{22}/\sigma_{11} = 1.0$
$k_{12} = 0.2 \quad p/p_{c1} = 0.0$
$\delta\varepsilon_{12}/\varepsilon_{11} = 2.0 \quad \omega_{12} = 1500$
$\frac{T}{T_{c1}}$
1.0
0.8
0.6
0.4
0.2
0.0
0.2
0.4
0.6
0.8
1.0
x_1 or x_2

Figure 9

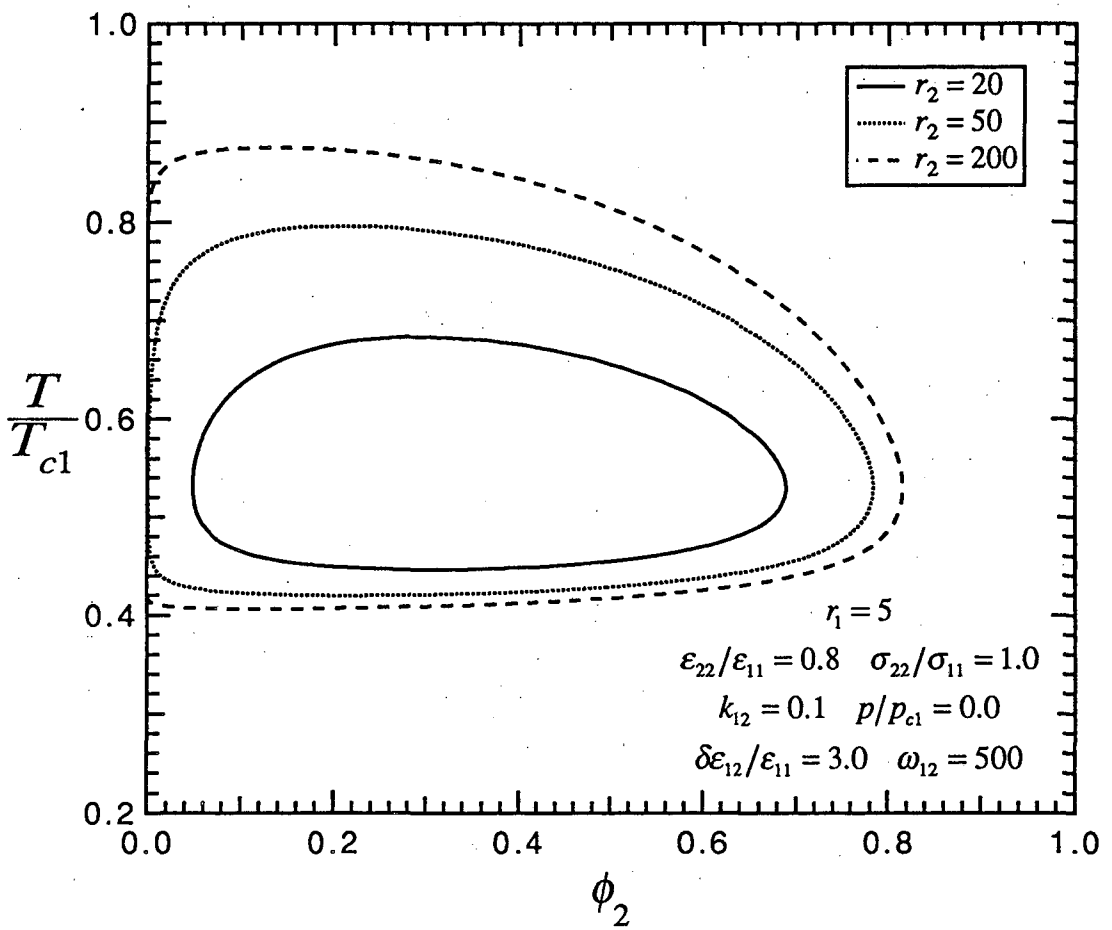
1.0
0.8
0.6
0.4
0.2
0.0
0.2
0.4
0.6
0.8
1.0
$\frac{T}{T_{c1}}$
ϕ_2
$r_2 = 20$
$r_2 = 50$
$r_2 = 200$
$r_1 = 5$
$\varepsilon_{22}/\varepsilon_{11} = 0.8 \quad \sigma_{22}/\sigma_{11} = 1.0$
$k_{12} = 0.1 \quad p/p_{c1} = 0.0$
$\delta\varepsilon_{12}/\varepsilon_{11} = 3.0 \quad \omega_{12} = 500$

LAWRENCE BERKELEY LABORATORY
UNIVERSITY OF CALIFORNIA
TECHNICAL INFORMATION DEPARTMENT
BERKELEY, CALIFORNIA 94720